1

2

3

4 **The *Helicobacter pylori* TlpD cytoplasmic chemoreceptor requires an intact C-terminus for polar**

5 **localization and function**

6 *Running title: TlpD requires the C-terminal 45 amino acids*

7 Raymondo Lopez-Magaña[a] & Karen M. Ottemann[a,#]

8

9

10 [a]Department of Microbiology and Environmental Toxicology, UC Santa Cruz, Santa Cruz, CA

11

12 [#]Corresponding author

13 Email: Ottemann@ucsc.edu

Abstract

Bacteria localize proteins to distinct subcellular locations, including chemoreceptors, which frequently localize to the bacterial pole. Although some polarity-promoting mechanisms have been described, many chemoreceptors lack clear routes to becoming polar. TlpD of the bacterial pathogen *Helicobacter pylori* is one such protein. This cytoplasmic chemoreceptor localizes to the pole in a manner that is independent of the other chemoreceptors. In this work, we evaluated the role of TlpD domains in its function. Truncated proteins were created that lacked different amounts of the N- or C-termini and expressed in *H. pylori* in place of native *tlpD* or as the sole chemoreceptor. These TlpD variants were examined for expression, protein localization, association with chemotaxis signaling proteins, and effect on motility. TlpD that lacked any portion of the N-terminal 104 amino acids did not produce detectable protein. In contrast, TlpD retained expression with loss of the C-terminal 45 amino acids. TlpD lacking the last 45 amino acids (TlpDΔC4) preserved the ability to interact with CheW and CheV proteins based on bacterial two-hybrid analysis but were unable to localize to the pole either on their own or in the presence of other chemoreceptors. TlpDΔC4 was found diffuse in the cytoplasm, and interacted with CheV1, CheV2, and CheV3 at this location but not CheW. TlpDΔC4 did not confer chemotactic abilities in soft agar chemotaxis assays. These findings suggest the C-terminal end of TlpD plays a previously unappreciated role in promoting TlpD polar localization and function.

Importance

Bacteria place their proteins in specific locations that are required for the proteins to function including the bacterial pole. How the bacterial cell identifies which proteins go to the pole is not fully understood. In this work, we dissect parts of a protein called TlpD that naturally goes to the pole. We find that mutants lacking one end of TlpD lose their polar placement, but retain other abilities. TlpD allows directed motility known as chemotaxis. This ability is critical for infection in *H. pylori* and numerous other pathogens. When TlpD loses its polar placement, the protein no longer functions for

38 chemotaxis, laying the foundation for future studies that can dissect how this segment promotes
39 function and eventually translate into therapies for *H. pylori* infection.

40 **Introduction**

41 *H. pylori* is a human pathogen that infects approximately one-half of the world's population (1).
42 This bacterium infects the stomach and causes chronic stomach inflammation and gastric cancer (1). To
43 reach the stomach, *H. pylori* must navigate a dynamic environment. En route, *H. pylori* encounters
44 various signals, including mammalian produced ones such as acid from stomach parietal cells and
45 reactive oxygen from epithelial and innate immune cells (2–5). One strategy *H. pylori* uses to circumvent
46 such harmful compounds and find beneficial ones is directed motility, also known as chemotaxis (6). The
47 chemotaxis signal transduction system, extensively studied in *Escherichia coli*, allows bacteria to sense
48 concentration gradients of particular chemicals and initiate a motility response (7–10). This chemotaxis
49 system is required for *H. pylori* to establish infection (2, 11–14). The ability to sense and mount an
50 appropriate response towards these signals allows effective navigation and infection.

51 The *H. pylori* chemotaxis system, like the *E. coli* one, operates as a multiprotein complex. Like
52 that of well-studied bacteria, this complex forms via protein-protein interactions, including between
53 sensors known as chemoreceptors that form interactions with coupling proteins and the CheA histidine
54 kinase, to control kinase activity (15–17). In contrast to the one-coupling protein system of *E. coli* that
55 uses the canonical coupling protein CheW, the chemotaxis system of *H. pylori* contains three additional
56 coupling proteins called CheV1, CheV2, and CheV3 (15, 18). These CheV paralogs are proposed to
57 function in several ways, including as coupling proteins, phosphate sinks, or possibly as unique coupling
58 proteins to accommodate chemoreceptors that cannot couple to CheW (15, 19, 20). In the *H. pylori*
59 system, both CheW and CheV1 are critical to build chemoreceptor arrays (16, 17) and each CheV plays

60 specific roles in motility (18, 21). However, the exact roles of CheV2 and CheV3 in *H. pylori* chemotaxis
61 have yet to be determined (15, 16).

62 The *H. pylori* chemotaxis system uses four chemoreceptors called TlpA, TlpB, TlpC, and TlpD.
63 TlpA, TlpB and TlpC are integral membrane proteins whereas TlpD is soluble, not membrane bound and
64 cytoplasmic (6, 22). This cytoplasmic chemoreceptor contains a C-terminal chemoreceptor zinc binding
65 (CZB) sensing domain (17, 23). Despite being cytoplasmic, TlpD localizes to the pole and retains this
66 capability even in the absence of any membrane bound chemoreceptors (17). However, the mechanism
67 by which TlpD locates to the cell pole remains unclear.

68 TlpD recruits other chemotaxis proteins to the cell pole. This chemoreceptor is sufficient to
69 recruit CheA, CheW, CheV1, and CheV3 proteins to the *H. pylori* cell pole (17). TlpD likely interacts with
70 the CheW and CheV coupling proteins via its methyl accepting (MA) domain, as has been shown in other
71 chemoreceptors. TlpD interacts directly with coupling proteins CheW and CheV1 (16). This interaction
72 with coupling proteins facilitates an indirect interaction with the CheA kinase to form a functional
73 signaling unit. Indeed, a combination of reconstituted TlpD, CheA and CheW or CheV1 proteins are
74 sufficient to drive CheA phosphorylation and suggest either coupling protein can work with TlpD to
75 create a functional signaling unit in vitro (16, 24). Moreover, *H. pylori* with TlpD as its only
76 chemoreceptor retains spreading motility on soft agar, indicative of chemotaxis function, and thus
77 supports a model by which TlpD alone forms an autonomous and functional signaling unit (17).

78 TlpD plays a key role in *H. pylori* infection. Numerous studies have shown that TlpD is required
79 for full stomach colonization in both mice and gerbils (2, 11, 25). Of the four *H. pylori* chemoreceptors,
80 *tlpD* mutants colonize less well than wild type or any isogenic chemoreceptor mutant (2, 11, 25).
81 Additionally, TlpD mounts a chemotactic response to reactive oxygen species including hydrogen
82 peroxide, superoxide and hypochlorous acid (17, 24). As all these signals are found during infection, it

83 makes sense that TlpD would be an important chemoreceptor. Indeed, TlpD was found to be expressed
84 in all tested *H. pylori* strains, suggesting it is retained to a higher degree than other chemoreceptors (17).
85 These findings highlight the importance of TlpD in the chemotaxis system of *H. pylori* for infection.

86 In this study, we evaluated the roles of parts of TlpD for which there is no known function. We
87 created TlpD truncations lacking portions of either the N or C terminus and analyzed how loss of these
88 sequences affected function in situ, expressing the proteins in the native *H. pylori*. Most truncations
89 resulted in loss of stability in *H. pylori* but one mutant construct, however, was stably expressed in *H.*
90 *pylori*: a C-terminus deletion of the last amino acids, 388-433. This region is C-terminal to the CZB
91 domain and based on bioinformatic analysis, had no detectable features or domains. This truncated
92 protein, called TlpDΔC4, maintained its ability to interact with CheW and CheV coupling proteins, based
93 on immunolocalization and bacterial two hybrid assays, but lost its ability to localize to the pole and
94 function.

95

96 **Results**

97 **Identification of TlpD domain endpoints to allow selective omission of unannotated regions**

98 Previous work had identified domains of TlpD (23, 24) but to define precise endpoints, we
99 carried out up-to-date bioinformatic analyses. AlphaFold2 (26) predicted the known MA and CZB
100 domains (23) and provided a predicted structure of the 433 amino acid TlpD protein (Fig. 1A). Alphafold2
101 defined the MA domain as amino acids 152 to 287 and the CZB domain from 315 to 379 (Fig. 1B).
102 Following the C-terminal CZB domain was a 54 amino acid stretch with no annotated domains (Fig. 1A
103 and B). The N-terminus comprised the first 140 amino acids and is predicted to orient perpendicular to
104 the rest of the protein (Fig. 1A and B). Like the C-terminus, the N-terminal stretch had no annotated
105 motifs (Fig. 1A). Further analysis using the bioinformatic servers MotifFinder, NCBI CDD, Protein CCD

106 similarly did not identify motifs in the N- or C-terminal regions (27–29) (Fig. S1 and File S1). Secondary
107 structure analysis using Globplot (30) determined that these regions, along with most of TlpD, were
108 structured (Fig. S1). Overall, these analyses suggest that TlpD has known domains in the middle portion,
109 while the N- and C-termini are predicted to be folded into secondary structures but any lack identifiable
110 domains.

111 Because it is unclear what the functions of the TlpD N- or C-terminus are, we took advantage of
112 the two-domain architecture of TlpD to create truncated versions that removed select regions but
113 retained the MA or CZB domains (Fig. 1B). An initial round of constructs did not carefully avoid predicted
114 secondary structure endpoints and resulted in proteins that were not expressed in *H. pylori* (Fig. S2). In
115 the second round, predicted secondary structure endpoints were avoided and a 3X FLAG tag was added
116 to improve detection (File S1 and S2). We designed these constructs to integrate into the non-essential
117 *rdxA* locus of *H. pylori*, facilitated by an erythromycin resistance marker for positive selection and
118 flanking *rdxA* sequences (Fig. S3A), in single copy under the control of the *tlpD* promoter (Table 1).

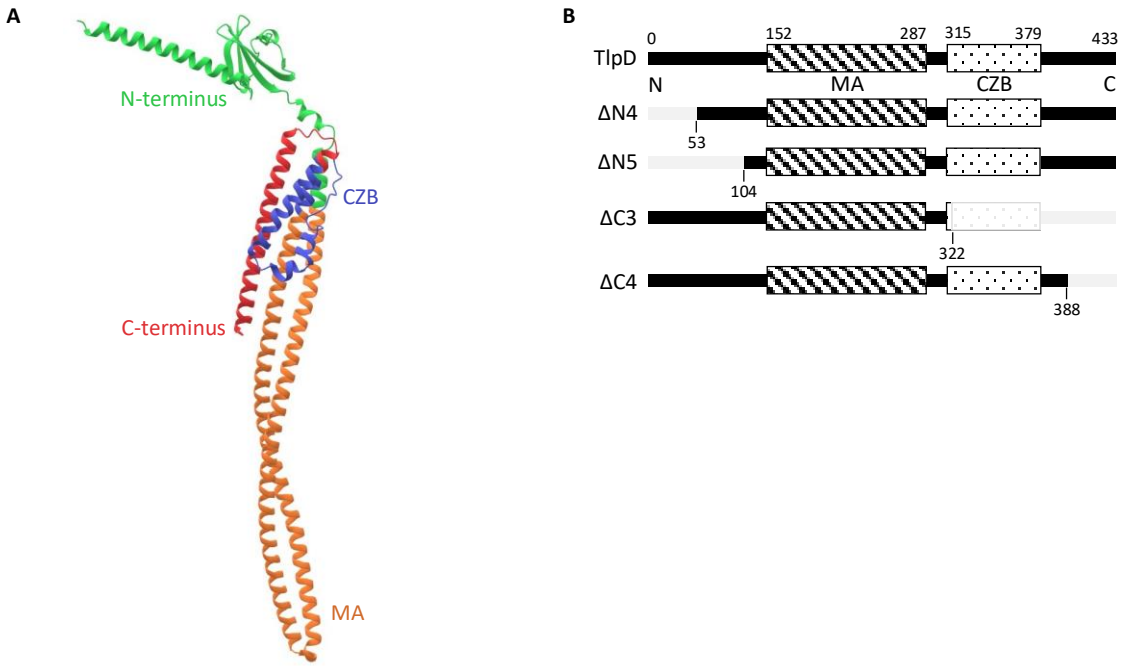

119

120 **Figure 1. *H. pylori* TlpD predicted structure and domains.** (A) AlphaFold predicted structure of *H. pylori*
121 TlpD. TlpD is 433 amino acids in length with two known domains, the MA domain (orange) and CZB
122 domain (blue). The region with no known domains at the N-terminus is shown in green, and at the C-
123 terminus in red. (B) Diagram of modified versions of *H. pylori* TlpD with domains and truncation sites
124 indicated (grey). TlpD represents the full-length version of the protein at 433 amino acids, ΔN4 is
125 truncated at residue 53, ΔN5 is truncated at residue 104, ΔC3 is truncated at residue 322, and ΔC4 is
126 truncated at residue 388. Each of these constructs contains a C-terminal 3xFLAG tag.

Table 1. Plasmids used in this study.

Plasmid	KO reference no.	Genotype/description	Reference/source
DH10B pTwist *tlpD 3xflag*	KO1926	*rdxA::tlpD 3xflag erm*	This study
DH10B pTwist *tlpDΔN4*	KO1927	*rdxA::tlpDΔN4 3xflag erm*	This study
DH10B pTwist *tlpDΔN5*	KO1928	*rdxA::tlpDΔN5 3xflag erm*	This study
DH10B pTwist *tlpDΔC3*	KO1929	*rdxA::tlpDΔC3 3xflag erm*	This study
DH10B pTwist *tlpDΔC4*	KO1930	*rdxA::tlpDΔC4 3xflag erm*	This study
DH10B pTwist *tlpD*	KO1936	*rdxA::tlpD erm*	This study
pUT18	KO1346	BACTH vector	(31); J. Gober, UCLA
pUT18C	KO1347	BACTH vector	(31); J. Gober, UCLA
pKT25-zip	KO1348	BACTH pos. control vector	(31); J. Gober, UCLA
pUT18C-zip	KO1349	BACTH neg. control vector	(31); J. Gober, UCLA
XL1-Blue pUT18C-*tlpD*	KO1954	BACTH. G27 *tlpD* cloned on the C-terminus of pUT18C.	This study
XL1-Blue pUT18C-*tlpDΔC4*	KO1956	BACTH. G27 truncated *tlpDΔC4* cloned on the C-terminus of pUT18C.	This study
DH5a *cheV1*-pKNT25	KO1432	BACTH. G27 *cheV1* cloned on the N-terminus of pKNT25	(16)

DH5a *cheW*-pKTN25	KO1434	BACTH. G27 *cheW* cloned on the N-terminus of pKNT25	(16)

127

Table 2. Bacterial strains used in this study.

Strain	KO reference no.	Genotype/description	Reference/source
G27	KO379		(32), Nina Salama
G27 *ΔtlpD*	KO1165	*rdxA::kan-sac ΔtlpD::cat*	(33)
G27 *ΔtlpD, rdxA::tlpD 3xflag*	KO1931	KO1165 transformed with pTwist *tlpD 3xflag*	This study
G27 *ΔtlpD, rdxA::tlpDΔN4*	KO1932	KO1165 transformed with pTwist *tlpDΔN4*	This study
G27 *ΔtlpD, rdxA::tlpDΔN5*	KO1933	KO1165 transformed with pTwist *tlpDΔN5*	This study
G27 *ΔtlpD, rdxA::tlpDΔC3*	KO1934	KO1165 transformed with pTwist *tlpDΔC3*	This study
G27 *ΔtlpD, rdxA::tlpDΔC4*	KO1935	KO1165 transformed with pTwist *tlpDΔC4*	This study
*m*G27	KO625	Mouse adapted G27	(34)
mG27 ΔtlpD	KO1006	KO625 *ΔtlpD::cat*	(35)
*m*G27 *ΔABCD*	KO1021	*ΔtlpA ΔtlpB ΔtlpC::aphA3 ΔtlpD::cat*	(17, 36)
*m*G27 *ΔABCD, rdxA::tlpD*	KO1940	KO1021 transformed with pTwist *tlpD*	This study
*m*G27 *ΔABCD, rdxA::tlpDΔC4*	KO1941	KO1021 transformed with pTwist *tlpDΔC4 3xflag*	This study

128

129 **TlpD tolerates C-terminal but not the N-terminal truncations**

130 To evaluate the production of these TlpD truncation constructs in vivo, each *tlpD* construct was
131 transformed into *H. pylori* G27 *ΔtlpD* (Table 2), where they integrated into the genome at the *rdxA* locus
132 (Fig. S3A). Proper integration was confirmed by PCR using primers that flank the *rdxA* locus (Fig. S3B). We

133 then evaluated protein expression in *H. pylori* whole cell lysates by western blotting using an anti-FLAG
134 antibody, as used in *E. coli* (Fig. 2). For this approach, *H. pylori* strains were grown on standard solid
135 media (CHBA), scraped from the plate, normalized to a standard OD_{600} and lysed in Laemmli buffer. Full-
136 length TlpD (TlpD) was detected when expressed from the *rdxA* locus (Fig. 2), but strains expressing the
137 truncated variants showed variable expression. N-terminus truncated proteins (TlpD ΔN4 and ΔN5) had
138 little or no protein detected (Fig. 2). Strains expressing C-terminus truncated proteins (TlpD ΔC3 and ΔC4)
139 varied in the amounts of protein detected: TlpDΔC3 had a low signal, similar to TlpDΔN5, while TlpDΔC4
140 had a clearly detectable signal that was approximately half that of WT TlpD (Fig. 2). These findings
141 suggest the C-terminal end of TlpD can be removed with modest effect on protein expression, and this
142 protein was chosen for further characterization.

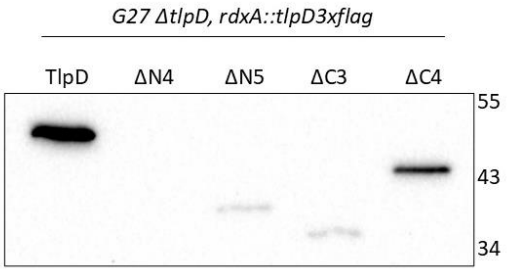

143

144 **Figure 2. Analysis of expression of TlpD WT and truncated variants expressed from *H. pylori rdxA*.**
145 Western blot of *H. pylori* G27 Δ*tlpD* strains complemented with *tlpD* constructs were analyzed from
146 whole-cell lysates with an anti-FLAG antibody, which recognizes the C-terminal tag. The TlpD variant
147 expressed is indicated at the top, with TlpD indicating full length with the 3XFLAG. Marker sizes are given
148 in kilodaltons on the right. The expected size of TlpD is 51 kDa, ΔN4 is 45 kDa, ΔN5 is 39 kDa, ΔC3 is 38
149 kDa, and ΔC4 is 45 kDa. Western blot is representative of 3 biological replicates.

150

151 **C-terminus truncated TlpDΔC4 retains interaction with CheV1 and CheW**

152 TlpDΔC4 was next analyzed for its ability to fold. TlpD interacts with chemotaxis proteins
153 including coupling proteins CheV and CheW (17). We therefore analyzed whether these interactions
154 were retained for TlpDΔC4 using an approach previously used with *H. pylori* CheV1 and CheW, the
155 bacterial two-hybrid (BACTH) analysis (16). Truncated *tlpD* was fused to the T18C fragment at the C-
156 termini (T18C-*tlpD*, T18C-*tlpDΔC4*), as done for full-length *tlpD*, and then *tlpD*ΔC4 plasmids were
157 analyzed with NT25 fragment plasmids with *cheV1* (*cheV1*-NT25) or *cheW* (*cheW*-NT25) (Fig. 3A) used
158 previously (16). TlpDΔC4 was able to interact with both CheV1 and CheW (Fig. 3B) to levels that were
159 significantly above the negative control. These levels are low but similar to ones obtained with full-length
160 TlpD here (Fig. 3) and as reported previously (16). This result supports that the truncated TlpDΔC4
161 retains binding function with both CheV1 and CheW, suggesting the TlpDΔC4 MA domain is correctly
162 folded.

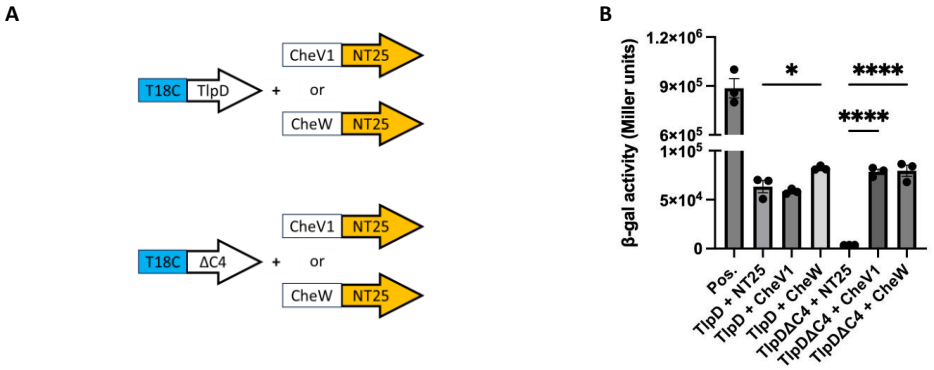

163

164 **Figure 3. TlpD's interaction with chemotaxis proteins is retained when the C-terminus is truncated.**
165 BACTH β-galactosidase (β-gal) assays of full-length and truncated (TlpDΔC4) TlpD with CheV1 and CheW.
166 (A) Diagrams of constructs used. (B) β-gal assays. Positive (+) controls are T25-zip and T18-zip. Negative (-
167) controls are the respective TlpD construct with blank T25 plasmids. β-gal activity is calculated from

168 three technical replicates with error bars indicating the standard error of the mean. *p < .05, ****p <

169 .0001.

170

171 **TlpDΔC4 is unable to localize to the *H. pylori* cell pole**

172 TlpD normally localizes to the *H. pylori* pole even when it is the only chemoreceptor present

173 (17). We next analyzed the localization of TlpDΔC4 using immunofluorescence when it was expressed in

174 either the presence of other chemoreceptors (TlpA, TlpB) or as the sole chemoreceptor. Western blot

175 analysis of the receptorless *H. pylori* strain (Δ*ABCD*) complemented with TlpD shows protein expression

176 (Fig. S4). Full-length TlpD localized to the pole in the presence or absence of the other chemoreceptors,

177 as previously shown for a strain of *H. pylori* with natively expressed TlpD (17) (Fig. 4A and B). In contrast,

178 TlpDΔC4 was diffuse throughout the bacterium's cell cytoplasm (Fig. 4A). This cytoplasmic localization

179 did not change when the other chemoreceptors were present (Fig. 4B). Altogether, using two different *H.*

180 *pylori* strain backgrounds, these findings support the finding that the C-terminal portion of TlpD is

181 important for polar localization.

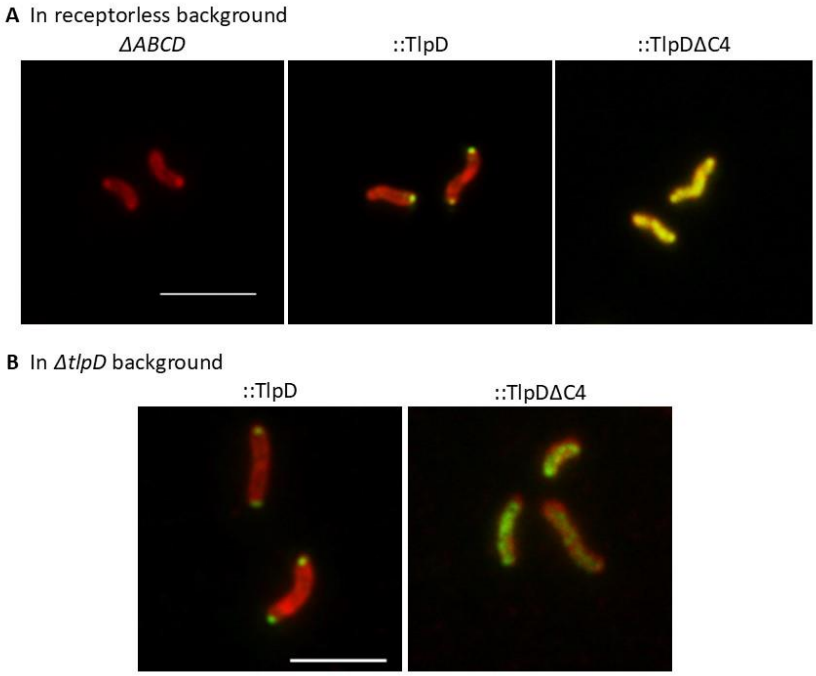

182

183 **Figure 4. TlpD is polar when the C-terminus is intact and diffused when the C-terminus is disrupted.**
184 Immunolocalization of *H. pylori* whole cells producing full-length TlpD or truncated TlpDΔC4 protein. *H.*
185 *pylori* was detected with chicken anti-*H. pylori* followed by goat anti-chicken conjugated to AlexaFluor
186 594 (red). TlpD proteins indicated above each image were detected with preabsorbed rabbit anti-TlpA22
187 (Δ*ABCD*, TlpD) or rat anti-FLAG (TlpD, ΔC4) followed by goat anti-rabbit or goat anti-rat conjugated to
188 AlexaFluor 488 (green). Scale bar = 4µM. Images are representative of 3 biological replicates, with 20-50
189 bacterial cells analyzed for each sample.

190 **TlpDΔC4 alters localization of chemotaxis coupling proteins CheV1, CheV2, and CheV3 but not**
191 **CheW**

192 The above results show that TlpDΔC4 retains ability to interact with chemotaxis coupling
193 proteins (Fig. 3) but mislocalizes (Fig. 4). The CheV and CheW coupling proteins normally are localized at
194 the cell pole in *H. pylori* by interactions with the chemoreceptor complex (16, 17). We next analyzed how
195 TlpDΔC4 would affect localization of these *H. pylori* chemotaxis signaling proteins, using strains that

196 retained the TlpA and TlpB chemoreceptors and antibodies previously shown to be specific to each
197 coupling protein (17, 36). Full-length TlpD expression resulted in all CheV and CheW proteins being
198 entirely polar, with no detectable cytoplasmic staining, as previously shown with wild type *H. pylori* (17)
199 (Fig. 5). In contrast, when TlpDΔC4 was expressed, CheV1, CheV2, and CheV3 displayed both polar and
200 nonpolar staining, with CheV3 showing the most diffused cytoplasmic signal (Fig. 5). CheW, in
201 comparison, showed only polar staining. These results further support that TlpDΔC4 retains the ability to
202 interact with chemotaxis coupling proteins and can retain them in the cytoplasm.

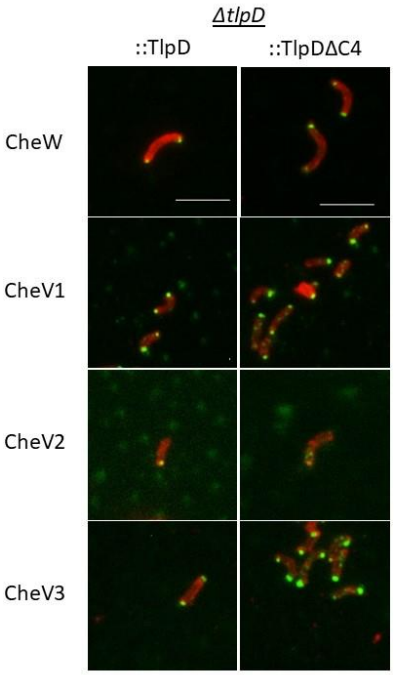

203

204 **Figure 5. Localization of CheW and CheV coupling proteins in *H. pylori* in the presence of TlpDΔC4.**
205 Immunolocalization of *H. pylori* chemotaxis proteins CheW, CheV1, CheV2, and CheV3 in whole cells
206 producing full-length (TlpD-FLAG) or truncated (TlpDΔC4-FLAG) protein. *H. pylori* was detected with
207 chicken anti-*H. pylori* followed by goat anti-chicken conjugated to AlexaFluor 594 (red). Individual
208 chemotaxis proteins indicated on the left were detected with preabsorbed guinea pig anti-CheW, rabbit
209 anti-CheV1, rabbit anti-CheV2 or rabbit anti-CheV3 followed by goat anti-guinea pig or goat anti-rabbit

210 conjugated to AlexaFluor 488 (green). Scale bar = 4µM. Images are representative of 3 biological
211 replicates, with 20-50 bacterial cells analyzed for each sample.

212

213 **TlpDΔC4 does not confer soft agar migration in *H. pylori***

214 To explore TlpDΔC4 function, chemotaxis ability of strains expressing TlpDΔC4 was analyzed
215 using a field-standard chemotaxis assay, migration in soft agar. In this assay, bacteria are inoculated at a
216 single point, and if motile and chemotactic, migrate outwards to form expanded colonies. Using strains
217 that express the *rdxA* copy of *tlpD* as their only chemoreceptor, we found that full-length TlpD was able
218 to confer spreading to diameters that were significantly elevated compared to the parent strain lacking
219 all chemoreceptors (*ΔABCD*) (Fig. 6A and C). These findings suggest that complementation of wild-type
220 *tlpD* in the *rdxA* locus is partially sufficient to restore spreading motility in *H. pylori*. The *tlpD*ΔC4
221 complemented strain, in contrast did not spread even after seven days (Fig. 6B and D). This finding
222 suggests that truncation of the C-terminus of TlpD results in a chemoreceptor that is insufficient to
223 restore spreading. These findings suggest that TlpDΔC4 may be unable to establish a working chemotaxis
224 system.

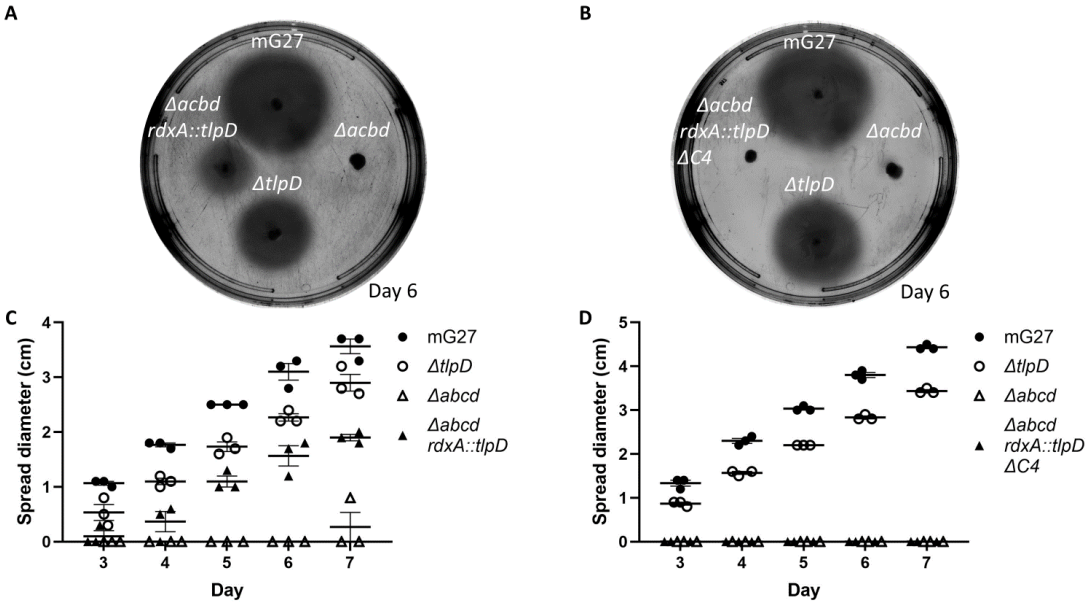

Figure 6. *H. pylori* that express TlpDΔC4 as the sole chemoreceptor do not spread on soft agar. (A) *H. pylori* wild-type mG27 and isogenic mutants were analyzed for chemotaxis by soft agar spreading. Strains were stabbed onto soft agar and spreading was measured after 3 days. Strains included are the parent *H. pylori* lacking all chemoreceptors (*ΔABCD,* called *Δabcd* here), and isogenic versions complemented with a full-length TlpD (*rdxA::tlpD*) (A) or with TlpDΔC4 (*rdxA::tlpD ΔC4*) (B). Plates are representative of 3 biological replicates, with three technical triplicates. Error bars represent the standard error of the mean.

Discussion

Our experiments with a truncated version of the cytoplasmic protein TlpD revealed that TlpD polar localization requires its C-terminal 45 amino acids. We reached this conclusion using immunofluorescence of FLAG-tagged full length TlpD or FLAG-tagged TlpDΔC4. Full length TlpD-FLAG localized to the pole as reported for TlpD lacking the FLAG (17), suggesting the FLAG tag did not disrupt any localization signals, as seen with a previous V5 tag (37). TlpDΔC4-FLAG, in contrast, did not display polar localization, suggesting that the C-terminal 45 amino acids are critical for localization directly or for

240 allowing TlpD to adopt a form that can localize. Our analysis furthermore suggests that the TlpDΔC4
241 protein can fold, based on its ability to maintain interactions with CheV proteins in *H. pylori* and CheV1
242 and CheW in the BACTH assays. Interestingly, CheV proteins mislocalized to the cytoplasm more than
243 CheW did when TlpDΔC4 was present, suggesting that TlpD might have an interaction preference for
244 CheV proteins versus CheW, as suggested by previous BACTH studies of TlpD (16) and seen in
245 *Campylobacter jejuni* chemoreceptors (38). Overall, these findings support the new idea that TlpD
246 requires its C-terminal 45 amino acids to properly localize.

247 Our search to identify features within the C-terminal 45 amino acids of TlpD revealed no
248 apparent hits. The AlphaFold structure described here suggests that this region adopts an extended 43
249 amino acid alpha helix that sits alongside the MA and CZB domains on one side, leaving the other side
250 exposed on the surface (Fig. 1A). Similarly, it is possible that the N and C-termini of TlpD interact with
251 one another, based on the idea that it was difficult to truncate either region. Thus, this region is clearly
252 important but not yet clear whether it plays a structural, regulatory or protein-protein interaction
253 function.

254 A potential function of this C-terminal stretch is in promoting protein-protein interactions.
255 Previous work showed that TlpD's polar localization was dynamic, with TlpD residing at the pole under
256 conditions that correlated with high energy, and diffuse in conditions correlated with low ATP (25, 37).
257 Besides the chemotaxis signaling proteins, several other proteins have been identified to interact with
258 TlpD. Yeast two-hybrid analyses identified TlpD interactors as acetone carboxylase (AcxC, HP0599) (39)
259 and sialic acid binding protein (HP0721) (40, 41). Two additional proteins, aconitase (AcnB) and catalase
260 (KatA) were shown to interact with TlpD based on pull downs from *H. pylori* extracts (37). AcnB, KatA,
261 and AcxC were further studied for their ability to localize TlpD to the pole by analyzing TlpD position in
262 mutants lacking the genes for each protein. Loss of *katA* resulted in TlpD being less polar, and observed
263 throughout the cell body (37). Whether TlpD interacts directly with KatA and via which regions is not

264 known. This work however corroborates that TlpD is polarly localized in a manner that is regulated and
265 via specific protein-protein interactions beyond the chemotaxis signaling network.

266 TlpD plays a critical role in building the chemotaxis protein arrays. Previous work had shown that
267 TlpD as the sole chemoreceptor localizes to the pole, and is sufficient to localize the main components of
268 the chemotaxis signaling complex—CheA, CheW, CheV1 and CheV3 to the cell pole too (17).
269 Furthermore, work with *H. pylori* that expressed only one transmembrane chemoreceptor, either TlpA or
270 TlpB, and lacked TlpD, mislocalized all three CheV proteins (42). These studies suggest TlpD plays a
271 critical role in promoting chemotaxis proteins to localize to the pole. Our localization studies showed
272 that even when using an *H. pylori* strain that retained TlpA and TlpB, two transmembrane
273 chemoreceptors, the TlpDΔC4 was not at the pole and mislocalized CheV proteins (Fig. 5). These findings
274 suggest that transmembrane chemoreceptors of *H. pylori* are not sufficient to maintain a distinctly polar
275 chemotaxis complex, but rather require polar TlpD.

276 These findings provide insight into the workings of cytoplasmic chemoreceptor proteins. The
277 cytoplasmic chemoreceptors that localize to the cell pole do so by colocalization with transmembrane
278 chemoreceptors (43–45), and in some cases switch between a diffused cytoplasmic protein and a distinct
279 polar topology (37, 46). Cytoplasmic chemoreceptors presumably utilize similar mechanisms as those
280 used by other proteins to drive polar localization including stochastic self-assembly, interaction with
281 polar anchor proteins, or interactions with plasmid partitioning homologues (47). TlpD contains a CZB
282 domain, and our findings may be specific to these types of chemoreceptors. One candidate for
283 comparative analysis is the CZB-containing cytoplasmic chemoreceptor McpA (NCBI Ref Seq:
284 WP_000475246.1) from the enteric pathogen *Salmonella enterica*. McpA is a 352 amino acid
285 chemoreceptor protein with an identified MA domain, a C-terminal CZB domain, and an N-terminal
286 coiled coil (48, 49). *S. enterica* that lacks seven of its nine chemoreceptors, retaining only McpA and
287 another of unknown function called Tip, fail to spread on soft agar (50, 51). McpA was not the focus of

288 these previous studies, however the findings do suggest this protein is not sufficient to confer a
289 spreading phenotype in *S. enterica*. The alignment of full length TlpD and McpA shows 33% amino acid
290 identity over the entire protein, and the C-terminal domains share 29% amino acid identity. Moreover,
291 McpA retains the conserved CZB motif (**H**xx[WFYL]x_{21-28}**C**x[LFMVI]Gx[WFLVI]x_{18-27}**H**xxx**H**) at its C-terminus
292 (amino acids 246-303) (23). The localization of McpA is not yet known however and will be interesting
293 for future studies.

294 In sum, our work shows that TlpD supports building of a functional chemosensory complex at
295 the pole and relies on the sequences at its C-terminal end to accomplish this function. One model,
296 consistent with our data, is that the C-terminus of TlpD interacts with an as-yet-identified polar landmark
297 protein, to bring TlpD to the pole, possibly via catalase. Once there, TlpD plays a critical role in nucleating
298 chemosensory array formation. Testing this model and exploring whether other cytoplasmic
299 chemoreceptors have similar localization sequences is an exciting area for future work.

300 Materials and Methods

301 **Bacterial strains and growth conditions.** All *H. pylori* and *E. coli* strains used in this study are listed in
302 Tables 1 and 2. *H. pylori* was grown on Columbia Horse Blood Agar (CHBA) containing 5% (vol/vol)
303 defibrinated horse blood (Hemostat Labs, Davis, CA), 0.2% (wt/vol) β-cyclodextrin (TCI), 5 µg/mL
304 cefsulodin (Sigma Aldrich), 50 µg/mL cycloheximide (GoldBio), 2.5 U/mL polymyxin B (Sigma Aldrich) and
305 10 µg/mL vancomycin (GoldBio). For the selection of *H. pylori* mutants, 13 µg/mL chloramphenicol, 15
306 µg/mL kanamycin (Fisher BioReagents), or 25 µg/mL erythromycin (GoldBio) was used. For liquid
307 cultures, *H. pylori* was grown with brucella broth containing 10% heat-inactivated fetal bovine serum
308 (Gibco) (BB10). Cultures were incubated at 37°C in microaerobic conditions (5% O_2, 10% CO_2, and 85%
309 N_2). *E. coli* was grown on LB media containing 100 µg/mL ampicillin or 30 µg/mL kanamycin (Fisher
310 BioReagents) and incubated at 37°C unless otherwise stated.

311 **Strategy for creation of truncated TlpD.** To construct truncated versions of G27 TlpD (Uniprot:B5Z6X0),
312 Protein CCD (29) was used to identify predicted secondary structures, features, and domains within the
313 protein and served as the basis for selecting truncation sites that avoid secondary structures and
314 predicted or known regions. TlpD N-terminal truncations at amino acids 53 (ΔN4) and 104 (ΔN5), were
315 selected to sit in between secondary structures. The TlpD C-terminus truncations at amino acids 322
316 (ΔC3) and 388 (ΔC4) were selected to abolish or retain the CZB domain without interrupting the
317 canonical MA domain, respectively. Additionally, 200bp upstream of *tlpD* was included to capture any
318 transcriptional regulatory sites and sequences encoding a 3xFLAG tag (DYKDDDDK-DYKDDDDK-
319 DYKDDDDK) was added to the C-terminus of TlpD. Lastly, an erythromycin resistance gene and its
320 promoter were added for positive selection, downstream of *tlpD*. This entire sequence was flanked by
321 500bp upstream and downstream of the non-native locus, *rdxA*, for chromosomal integration in *H.*
322 *pylori*. pTwist Amp High Copy plasmids with ampicillin resistance were ordered from Twist Bioscience
323 that contained these *tlpD* cassette sequences (File S2). These plasmids were then transformed into
324 electrocompetent *E. coli* DH10B cells using ampicillin selection followed by single colony purification.

325 **Creation of G27 and mG27 *tlpD* complement mutants.** For transformation into *H. pylori*, plasmids
326 containing *tlpD* sequences were purified from *E. coli* DH10B cells using the QIAprep Spin Miniprep Kit
327 (Qiagen) and added to a suspension of BB10 and 1-day old *H. pylori* G27 *ΔtlpD* or *ΔtlpA ΔtlpB ΔtlpC ΔtlpD*
328 cells from a CHBA plate (52). Transformants were selected by growth on CHBA containing 25 µg/mL
329 erythromycin followed by single colony purification. All mutations were verified using PCR with primers
330 that flank *rdxA* (*rdxA* Fwd and Rev) (Table S1).

331 **Western blot.** The expression of modified TlpD was observed by western blot. Liquid overnights of *E. coli*
332 were grown and used to prepare lysate samples. 1-to-2-day old *H. pylori* grown on CHBA solid media
333 containing erythromycin were resuspended in 1X Phosphate-Buffered Saline (PBS) and used to prepare
334 lysate samples. To prepare the lysate, samples were back diluted to OD_{600} = 0.7 in 200 µL. 6X SDS PAGE

335 sample buffer was added to the mixture at 1X final concentration and 1X PBS was added to 200 µL. Next,
336 samples were heated at 95-100°C for 10 minutes then placed on ice. Samples were electrophoresed on
337 10% or 12% SDS-PAGE gels then semi-dry transferred to polyvinylidene (PVDF) membranes using a trans-
338 blot SD semi-dry transfer cell (Bio-Rad). Relative protein loading was visualized by staining the
339 membrane with Direct Blue 71 (DB71) stain containing 0.008% DB71 (Sigma Aldrich) in 40% EtOH and
340 10% acetic acid prior to antibody binding. PVDF membranes were incubated with a 1:20,000 dilution of
341 rat anti-FLAG monoclonal antibody (Novus Biological, NBP1-06712) or a 1:4,000 to 1:10,000 dilution of
342 rabbit anti-TlpA22 antibody (33) diluted in 5% BSA at 4°C overnight. Membranes were next incubated
343 with a 1:20,000 dilution of horseradish peroxidase-conjugated goat anti-rat (R&D Systems) or a 1:10,000
344 dilution of goat anti-rabbit (Santa Cruz Biotechnology) secondary antibody. For visualization, SuperSignal
345 West Pico PLUS Chemiluminescent Substrate (Thermo Scientific) was added at a 1:1 ratio for 30 to 120
346 seconds with shaking at room temperature. Blots were then imaged using a Bio-rad Chemi-doc.

347 **Soft-agar motility assay.** *H. pylori* spreading motility was carried out as previously described (17, 53–55).
348 Briefly, soft agar plates were made with brucella broth and 0.35% bacto agar (BD). Soft agar was cooled
349 to 50°C before 2.5% heat-inactivated fetal bovine serum, 8 µg/mL amphotericin B, 5 µg/mL cefsulodin,
350 50 µg/mL cycloheximide, 2.5 U/mL polymyxin B, 5 µg/mL trimethoprim (Sigma Aldrich), and 10 µg/mL
351 vancomycin were added. Plates set for 3 days at room temperature before use. 1–2-day old *H. pylori*
352 strains from CHBA plates were inoculated halfway into the agar using a pipet tip. Plates were incubated
353 right side up in the 37°C microaerobic chamber and migration diameter was measured daily. mG27,
354 mG27 *ΔtlpD*, and mG27 *ΔtlpA ΔtlpB ΔtlpC ΔtlpD* were used as controls. Statistical analysis was done on
355 GraphPad Prism v9.4.1.

356 **Immunofluorescence.** Immunolocalization of *H. pylori* chemotaxis proteins TlpD, CheW, CheV1, CheV2,
357 and CheV3 was performed as previously described (17, 36). Briefly, 1-day old *H. pylori* grown on
358 Columbia Horse Blood Agar (CHBA) under microaerobic conditions was harvested and resuspended in

359 1mL of 1X PBS. 20 µL of the cell suspension was placed on a Poly-Lysine glass slide (Fisher Scientific) and
360 fixed with 0.075M $NaPO_4$ adjusted to pH7.4, 0.0025M NaCl and 2% paraformaldehyde (EMS) solution
361 then permeabilized in 3% Bovine Serum Albumin (BSA) (Millipore), 1% Saponin (Calbiochem), 0.01%
362 Triton X-100 and 0.02% Na Azide (Sigma Aldrich) resuspended in 1X PBS. The samples were blocked with
363 3% BSA and 0.01% Triton X-100 resuspended in 1X PBS solution. Samples were next treated with a 1:500
364 dilution of chicken anti-*H.pylori* (Agrisera AB), a 1:2,000 dilution of rat anti-FLAG (Novus Biological,
365 NBP1-06712), a 1:200 of preabsorbed or non-preabsorbed rabbit anti-TlpA22, or a 1:50 dilution of
366 preabsorbed rabbit anti-CheV1 (36), anti-CheV2, anti-CheV3 (J. Castellon, P. Lertsethtakarn, and K.M.
367 Ottemann, unpublished), or guinea pig anti-CheW (17) diluted in permeabilization solution (described
368 above). The anti-TlpA22, anti-CheV1, anti-CheV2, and anti-CheV3 antibodies were previously shown to
369 be specific to each coupling protein (17, 36). The samples were then treated with a 1:500 dilution of goat
370 anti-chicken Alexa Fluor 594 (Invitrogen, A11042) and goat anti-rat Alexa Fluor 488 (ThermoFisher,
371 A48262) or a 1:300 dilution of goat anti-rabbit Alexa Fluor 488 (Invitrogen, A11008) or goat anti-guinea
372 pig Alexa Fluor 488 (Invitrogen, A11073) diluted in permeabilization solution. The samples were washed
373 with blocking solution (described above) 3 times, a drop of Vectashield (Vector Laboratories) was added
374 to the cells and then sealed with coverslips. Fluorescence microscopy, using the Nikon Eclipse E600 was
375 used to visualize immunofluorescent cells at 100X objective with oil immersion. Texas Red and Fitc/GFP
376 filters were used to separately view and capture emission spectra from Alexa Fluor 594 (red) and 488
377 (green), respectively. Images were captured using a Hamamatsu ORCA-285 digital camera equipped to
378 the microscope. Fluorescent images were pseudo colored using ImageJ and merged using Adobe
379 Photoshop version 24.1.0. Scale = 4 µm. Images are representative of 3 biological replicates.

380 **Creation of Bacterial Two-hybrid (BACTH) plasmids and BACTH analysis.** Synthetic plasmid DNA from *E.*
381 *coli* DH10B was extracted using the Qiaprep Mini Kit (Qiagen). *H. pylori* G27 full-length *tlpD* and
382 truncated *tlpDΔC4* constructs were amplified using PCR with primers that amplify each sequence (*tlpD*

383 pUT18 Fwd and Rev, *ΔC4* pUT18 Fwd and Rev) (Table S1). The PCR products encoded PstI and SacI
384 restriction sites which were digested with Pst1-HF (NEB) and SacI-HF (NEB) restriction enzymes. BACTH
385 plasmids pUT18 and pUT18C (J. Gober, UCLA) (31) were similarly digested followed by phosphatase
386 treatment using rSAP following the manufacturer's suggested protocol (NEB). Treated PCR products and
387 plasmids were purified using the GFX PCR DNA and Gel Band Purification Kit (Cytiva). The purified
388 products were ligated using T4 DNA ligase following the manufacturer's suggested protocol (NEB) and
389 subcloned into electrocompetent *E. coli* XL1-Blue cells and ampicillin resistant colonies were selected. All
390 constructs were confirmed using PCR with the same primers used to amplify *tlpD* or *tlpDΔC4* (Table S1)
391 and DNA sequencing (Azenta).

392 Recombinant plasmids encoding the *cheV1*-NT25 (16), *cheW*-T25 (16), T18C-*tlpD*, T18C-*tlpDΔC4* and
393 were co-transformed, at 40 ng each, into electrocompetent BTH101 and plated on LB containing 40
394 µg/mL X-gal (5-bromo-4-chloro-3-ondolyl-beta-galacto-pyranoside) (GoldBio), 0.5 mM IPTG (Isopropyl β-
395 d-1-thiogalactopyranoside) (Fisher BioReagents), 100 µg/mL ampicillin, and 50 µg/mL kanamycin. As
396 positive controls, T25-zip and T18-zip plasmids were co-transformed into BTH101. As negative controls,
397 each *tlpD* recombinant plasmid was co-transformed with a pKNT25 blank BACTH plasmids. For
398 interaction assays, colonies including controls grown on LB containing X-gal, IPTG, ampicillin, and
399 kanamycin at the above-mentioned concentrations were used to make overnights in LB with ampicillin
400 and kanamycin at the above concentrations. The following day, 20 µL of each overnight was dropped
401 onto LB plates containing X-gal, IPTG, ampicillin, and kanamycin as above. These spots were allowed to
402 dry at room temperature before the plates were incubated at 30°C for 24 hours. Images were captured
403 using an iPhone 14 Pro and a white light transilluminator (Fisher Scientific). Images are representative of
404 3 biological replicates.

405 **β-Galactosidase Assay.** To quantify BACTH interactions, β-galactosidase activity was measured as
406 previously described (16, 31). Briefly, transformants were grown in LB broth with ampicillin, kanamycin,

407 and IPTG at the above concentrations at 30°C overnight. Overnight cultures were back diluted to OD_{600}=
408 0.1 in LB broth with ampicillin, kanamycin, and IPTG then grown at 30°C until OD_{600} 0.3-0.7 was reached.
409 100 µL of each culture was mixed with 900 µL cold Z-Buffer (0.06M $Na_2HPO_4.7H_2O$, 0.04M $NaH_2PO_4.H_2O$,
410 0.01M KCl, 0.001M $MgSO_4.7H_2O$, adjusted to pH 7.0 and 0.05M β-mercaptoethanol was added fresh
411 before use) in triplicate and mixed by inversion. Next, 50 µL of 0.1% SDS and 100 µL of chloroform was
412 added to each sample followed by a 10 second vortex. The samples and fresh 4mg/mL ortho-
413 Nitrophenyl-β-galactoside (ONPG) (Thermo Scientific) (in 0.1M Phosphate Buffer solution (0.06M
414 $Na_2HPO_4.7H_2O$ and 0.04M $NaH_2PO_4.H_2O$ adjusted to pH 7.0) were incubated at 30°C for 5 minutes. 200
415 µL ONPG solution was added to samples, vortexed, and time was recorded. The samples were incubated
416 at 30°C until a yellow color appeared. The reactions were stopped by adding 500 µL Stop solution (1M
417 Na_2CO_3), time recorded, and samples centrifuged at room temperature and max speed for 5 minutes
418 before OD_{420} was measured. Miller units were calculated to determine β-galactosidase activity using the
419 following formula: 1000 x (OD_{420} / [time * vol. culture * OD_{600}]) (56). β-gal activity is one biological
420 replicate with three technical replicates per sample. Statistical analysis was done on GraphPad Prism
421 v9.4.1.

422 **Acknowledgements**

423 We thank Fitnat Yildiz, Carrie Partch, and Chad Saltikov for discussion and support. We also thank UCSC
424 STEM Diversity for their support, particularly Yulianna Ortega and Xingci Situ. We are grateful to past and
425 current Ottemann lab members for their continued support throughout this project, particularly Arturo
426 Valdez and Christina Yang. The described project was supported by the National Institute of Allergy and
427 Infectious Diseases (NIAID) grant RO1AI116946 to K.M.O. The funders had no role in study design, data
428 collection, and interpretation, or decision to submit the work for publication.

429 **References**

430 1. Malfertheiner P, Camargo MC, El-Omar E, Liou JM, Peek R, Schulz C, Smith SI, Suerbaum S. 2023.
431 Helicobacter pylori infection. Nat Rev Dis Prim 9.

432 2. Collins KD, Hu S, Grasberger H, Kao JY, Ottemann KM. 2018. Chemotaxis allows bacteria to
433 overcome host-generated reactive oxygen species that constrain gland colonization. Infect
434 Immun 86:IAI.00878-17.

435 3. Flint A, Stintzi A, Saraiva LM. 2016. Oxidative and nitrosative stress defences of Helicobacter and
436 Campylobacter species that counteract mammalian immunity. FEMS Microbiol Rev 40:938–960.

437 4. Grasberger H, El-Zaatari M, Dang DT, Merchant JL. 2013. Dual oxidases control release of
438 hydrogen peroxide by the gastric epithelium to prevent helicobacter felis infection and
439 inflammation in mice. Gastroenterology 145:1045–1054.

440 5. Handa O, Naito Y, Yoshikawa T. 2010. Helicobacter pylori: A ROS-inducing bacterial species in the
441 stomach. Inflamm Res 59:997–1003.

442 6. Johnson KS, Ottemann KM. 2018. Colonization, localization, and inflammation: the roles of H.
443 pylori chemotaxis in vivo. Curr Opin Microbiol 41:51–57.

444 7. Colin R, Sourjik V. 2017. Emergent properties of bacterial chemotaxis pathway. Curr Opin
445 Microbiol 39:24–33.

446 8. Parkinson JS, Hazelbauer GL, Falke JJ. 2015. Signaling and sensory adaptation in Escherichia coli
447 chemoreceptors: 2015 update. Trends Microbiol 23:257–266.

448 9. Porter SL, Wadhams GH, Armitage JP. 2011. Signal processing in complex chemotaxis pathways.
449 Nat Rev Microbiol 9:153–165.

450 10. Wadhams GH, Armitage JP. 2004. Making sense of it all: Bacterial chemotaxis. Nat Rev Mol Cell
451 Biol 5:1024–1037.

452 11. Rolig AS, Shanks J, Carter JE, Ottemann KM. 2012. Helicobacter pylori requires TlpD-driven
453 chemotaxis to proliferate in the antrum. Infect Immun 80:3713–3720.

454 12. Behrens W, Schweinitzer T, Bal J, Dorsch M, Bleich A, Kops F, Brenneke B, Didelot X, Suerbaum S,
455 Josenhans C. 2013. Role of energy sensor TlpD of helicobacter pylori in Gerbil colonization and

456 genome analyses after adaptation in the Gerbil. Infect Immun 81:3534–3551.

457 13. Foynes S, Dorrell N, Ward SJ, Stabler RA, McColm AA, Rycroft AN, Wren BW. 2000. Helicobacter
458 pylori possesses two CheY response regulators and a histidine kinase sensor, CheA, which are
459 essential for chemotaxis and colonization of the gastric mucosa. Infect Immun 68:2016–2023.

460 14. Terry K, Williams SM, Connolly L, Ottemann KM. 2005. Chemotaxis plays multiple roles during
461 Helicobacter pylori animal infection. Infect Immun 73:803–811.

462 15. Alexander RP, Lowenthal AC, Harshey RM, Ottemann KM. 2010. CheV: CheW-like coupling
463 proteins at the core of the chemotaxis signaling network. Trends Microbiol 18:494–503.

464 16. Abedrabbo S, Castellon J, Collins KD, Johnson KS, Ottemann KM. 2017. Cooperation of two
465 distinct coupling proteins creates chemosensory network connections. Proc Natl Acad Sci U S A
466 114:2970–2975.

467 17. Collins KD, Andermann TM, Draper J, Sanders L, Williams SM, Araghi C, Ottemann KM. 2016. The
468 Helicobacter pylori CZB cytoplasmic chemoreceptor TlpD forms an autonomous polar chemotaxis
469 signaling complex that mediates a tactic response to oxidative stress. J Bacteriol 198:1563–1575.

470 18. Pittman MS, Goodwin M, Kelly DJ. 2001. Chemotaxis in the human gastric pathogen Helicobacter
471 pylori: Different roles for CheW and the three CheV paralogues, and evidence for CheV2
472 phosphorylation. Microbiology 147:2493–2504.

473 19. Ortega DR, Zhulin IB. 2016. Evolutionary Genomics Suggests That CheV Is an Additional Adaptor
474 for Accommodating Specific Chemoreceptors within the Chemotaxis Signaling Complex. PLoS
475 Comput Biol 12:1–19.

476 20. Jiménez-Pearson MA, Delany I, Scarlato V, Beier D. 2005. Phosphate flow in the chemotactic
477 response system of Helicobacter pylori. Microbiology 151:3299–3311.

478 21. Lowenthal AC, Simon C, Fair AS, Mehmood K, Terry K, Anastasia S, Ottemann KM. 2009. A fixed-
479 time diffusion analysis method determines that the three cheV genes of Helicobacter pylori
480 differentially affect motility. Microbiology 155:1181–1191.

481 22. Collins KD, Lacal J, Ottemann KM. 2014. Internal Sense of Direction: Sensing and Signaling from
482 Cytoplasmic Chemoreceptors. Microbiol Mol Biol Rev 78:672–684.

483 23. Draper J, Karplus K, Ottemann KM. 2011. Identification of a chemoreceptor zinc-binding domain

484 common to cytoplasmic bacterial chemoreceptors. J Bacteriol 193:4338–4345.

485 24. Perkins A, Tudorica DA, Amieva MR, James Remington S, Guillemin K. 2019. Helicobacter pylori
486 senses bleach (HOCl) as a chemoattractant using a cytosolic chemoreceptor. PLoS Biol 17:1–33.

487 25. Schweinitzer T, Mizote T, Ishikawa N, Dudnik A, Inatsu S, Schreiber S, Suerbaum S, Aizawa SI,
488 Josenhans C. 2008. Functional characterization and mutagenesis of the proposed behavioral
489 sensor TlpD of Helicobacter pylori. J Bacteriol 190:3244–3255.

490 26. Jumper J, Evans R, Pritzel A, Green T, Figurnov M, Ronneberger O, Tunyasuvunakool K, Bates R,
491 Žídek A, Potapenko A, Bridgland A, Meyer C, Kohl SAA, Ballard AJ, Cowie A, Romera-Paredes B,
492 Nikolov S, Jain R, Adler J, Back T, Petersen S, Reiman D, Clancy E, Zielinski M, Steinegger M,
493 Pacholska M, Berghammer T, Bodenstein S, Silver D, Vinyals O, Senior AW, Kavukcuoglu K, Kohli
494 P, Hassabis D. 2021. Highly accurate protein structure prediction with AlphaFold. Nature
495 596:583–589.

496 27. Kanehisa M, Goto S, Kawashima S, Nakaya A. 2002. Thed KEGG databases at GenomeNet. Nucleic
497 Acids Res 30:42–46.

498 28. Marchler-Bauer A, Bo Y, Han L, He J, Lanczycki CJ, Lu S, Chitsaz F, Derbyshire MK, Geer RC,
499 Gonzales NR, Gwadz M, Hurwitz DI, Lu F, Marchler GH, Song JS, Thanki N, Wang Z, Yamashita RA,
500 Zhang D, Zheng C, Geer LY, Bryant SH. 2017. CDD/SPARCLE: Functional classification of proteins
501 via subfamily domain architectures. Nucleic Acids Res 45:D200–D203.

502 29. Mooij WTM, Mitsiki E, Perrakis A. 2009. ProteinCCD: Enabling the design of protein truncation
503 constructs for expression and crystallization experiments. Nucleic Acids Res 37:402–405.

504 30. Linding R, Russell RB, Neduva V, Gibson TJ. 2003. GlobPlot: Exploring protein sequences for
505 globularity and disorder. Nucleic Acids Res 31:3701–3708.

506 31. Karimova G, Pidoux J, Ullmann A, Ladant D. 1998. A bacterial two-hybrid system based on a
507 reconstituted signal transduction pathway. Proc Natl Acad Sci U S A 95:5752–5756.

508 32. Censini S, Lange C, Xiang Z, Crabtree JE, Ghiara P, Borodovsky M, Rappuoli R, Covacci A. 1996.
509 cag, a pathogenicity island of Helicobacter pylori, encodes type I-specific and disease-associated
510 virulence factors. Proc Natl Acad Sci U S A 93:14648–14653.

511 33. Williams SM, Chen YT, Andermann TM, Carter JE, McGee DJ, Ottemann KM. 2007. Helicobacter

512 pylori chemotaxis modulates inflammation and bacterium-gastric epithelium interactions in
513 infected mice. Infect Immun 75:3747–3757.

514 34. Castillo AR, Arevalo SS, Woodruff AJ, Ottemann KM. 2008. Experimental analysis of Helicobacter
515 pylori transcriptional terminators suggests this microbe uses both intrinsic and factor-dependent
516 termination. Mol Microbiol 67:155–170.

517 35. Rader BA, Wreden C, Hicks KG, Sweeney EG, Ottemann KM, Guillemin K. 2011. Helicobacter
518 pylori perceives the quorum-sensing molecule AI-2 as a chemorepellent via the chemoreceptor
519 TlpB. Microbiology 157:2445–2455.

520 36. Lertsethtakarn P, Howitt MR, Castellon J, Amieva MR, Ottemann KM. 2015. Helicobacter
521 pyloriCheZHP and ChePep form a novel chemotaxis-regulatory complex distinct from the core
522 chemotaxis signaling proteins and the flagellar motor. Mol Microbiol 97:1063–1078.

523 37. Behrens W, Schweinitzer T, McMurry JL, Loewen PC, Buettner FFR, Menz S, Josenhans C. 2016.
524 Localisation and protein-protein interactions of the Helicobacter pylori taxis sensor TlpD and
525 their connection to metabolic functions. Sci Rep 6:1–20.

526 38. Chandrashekhar K, Kassem II, Rajashekara G. 2017. Campylobacter jejuni transducer like
527 proteins: Chemotaxis and beyond. Gut Microbes 8:323–334.

528 39. Rain JC, Selig L, De Reuse H, Battaglia V, Reverdy C, Simon S, Lenzen G, Petel F, Wojcik J,
529 Schächter V, Chemama Y, Labigne A, Legrain P. 2001. The protein-protein interaction map of
530 Helicobacter pylori. Nature 409:211–215.

531 40. Bennett HJ, Roberts IS. 2005. Identification of a new sialic acid-binding protein in Helicobacter
532 pylori. FEMS Immunol Med Microbiol 44:163–169.

533 41. Hauser R, Ceol A, Rajagopala S V., Mosca R, Siszler G, Wermke N, Sikorski P, Schwarz F, Schick M,
534 Wuchty S, Aloy P, Uetz P. 2014. A second-generation protein-protein interaction network of
535 helicobacter pylori. Mol Cell Proteomics 13:1318–1329.

536 42. Castellón J. 2013. CheV1 Leads the Organization of Chemotaxis Signal Transduction Proteins in
537 Helicobacter pylori. UC St Cruz.

538 43. Bardy SL, Maddock JR. 2005. Polar localization of a soluble methyl-accepting protein of
539 Pseudomonas aeruginosa. J Bacteriol 187:7840–7844.

540 44. Meier VM, Scharf BE. 2009. Cellular localization of predicted transmembrane and soluble
541 chemoreceptors in Sinorhizobium meliloti. J Bacteriol 191:5724–5733.

542 45. Cannistraro VJ, Glekas GD, Rao C V., Ordal GW. 2011. Cellular stoichiometry of the chemotaxis
543 proteins in Bacillus subtilis. J Bacteriol 193:3220–3227.

544 46. Xie Z, Ulrich LE, Zhulin IB, Alexandre G. 2010. PAS domain containing chemoreceptor couples
545 dynamic changes in metabolism with chemotaxis. Proc Natl Acad Sci U S A 107:2235–2240.

546 47. Jones CW, Armitage JP. 2015. Positioning of bacterial chemoreceptors. Trends Microbiol 23:247–
547 256.

548 48. Frye J, Karlinsey JE, Felise HR, Marzolf B, Dowidar N, McClelland M, Hughes KT. 2006.
549 Identification of new flagellar genes of Salmonella enterica serovar typhimurium. J Bacteriol
550 188:2233–2243.

551 49. Schultz J, Milpetz F, Bork P, Ponting CP. 1998. SMART, a simple modular architecture research
552 tool: Identification of signaling domains. Proc Natl Acad Sci U S A 95:5857–5864.

553 50. Wang Q, Mariconda S, Suzuki A, McClelland M, Harshey RM. 2006. Uncovering a large set of
554 genes that affect surface motility in Salmonella enterica serovar typhimurium. J Bacteriol
555 188:7981–7984.

556 51. Lazova MD, Butler MT, Shimizu TS, Harshey RM. 2012. Salmonella chemoreceptors McpB and
557 McpC mediate a repellent response to L-cystine: A potential mechanism to avoid oxidative
558 conditions. Mol Microbiol 84:697–711.

559 52. Hu S, Giacopazzi S, Modlin R, Karplus K, Bernick DL, Ottemann KM. 2023. Altering under-
560 represented DNA sequences elevates bacterial transformation efficiency. MBio 14:1–6.

561 53. Ottemann KM, Lowenthal AC. 2002. Helicobacter pylori uses motility for initial colonization and
562 to attain robust infection. Infect Immun 70:1984–1990.

563 54. McGee DJ, Langford ML, Watson EL, Carter JE, Chen YT, Ottemann KM. 2005. Colonization and
564 inflammation deficiencies in Mongolian gerbils infected by Helicobacter pylori chemotaxis
565 mutants. Infect Immun 73:1820–1827.

566 55. Lowenthal AC, Hill M, Sycuro LK, Mehmood K, Salama NR, Ottemann KM. 2009. Functional
567 analysis of the Helicobacter pylori flagellar switch proteins. J Bacteriol 191:7147–7156.

56. Miller J. 1972. Experiments in molecular genetics. Cold Spring Harbor Laboratory. http://www.getcited.org/pub/101336765.

Supporting information

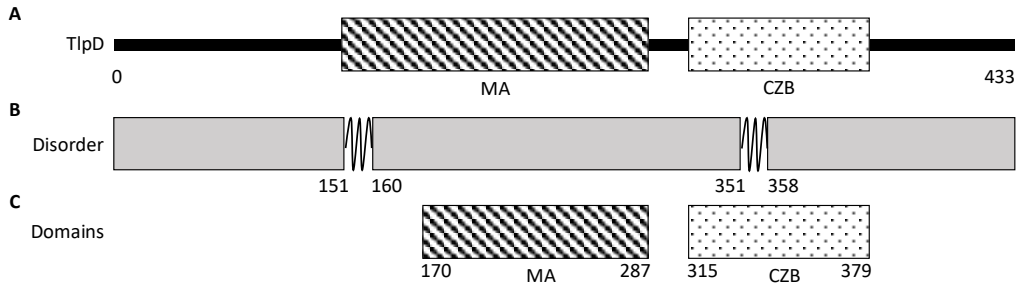

Figure S1. Summary of Predicted secondary structures and domains of TlpD. (A) Full-length TlpD for reference. (B) Predicted TlpD globular regions in grey and the unstructured regions shown as twists. (C) Predicted TlpD domains with the two highest scores, the MA and CZB domain.

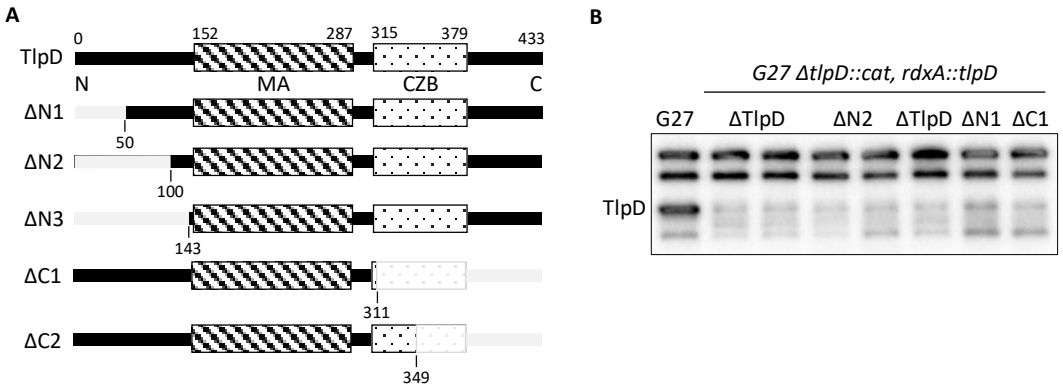

Figure S2. First generation of TlpD truncation constructs and expression in *H. pylori*. (A) Modified versions of *H. pylori* TlpD with domains and truncation sites (grey). TlpD is the full-length version of the protein at 433 amino acids, ΔTlpD are negative background controls, ΔN1 is truncated at residue 50, ΔN2 is truncated at residue 100, ΔN3 is truncated at residue 143, ΔC1 is truncated at residue 311, and ΔC2 is truncated at residue 349. (B) Western blot of *H. pylori* G27 strains with complemented *tlpD* constructs were analyzed from whole-cell lysates with an anti-TlpA-22 antibody (33) which recognizes the

582 conserved MA domain of all chemoreceptors. The expected size of wild-type TlpD is 48 kDa, ΔN1 is 42.9

583 kDa, ΔN2 is 37.4 kDa, and ΔC1 is 34 kDa. Western blots are representative of 3 biological replicates.

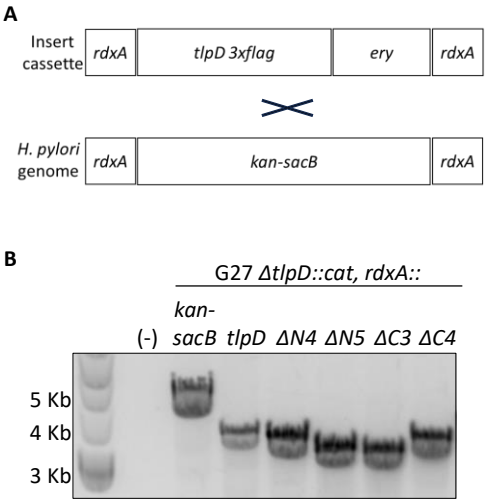

584

585 **Figure S3. *tlpD* sequence layout for transformation into the *H. pylori* genome.** (A) Design of *tlpD* insert

586 cassette for transformation into *H. pylori*. This cassette contains the *tlpD* sequence, a *3xflag* tag and

587 *erythromycin* (*ery*) resistance sequences that are flanked by *rdxA* homologous regions for integration

588 into the *H. pylori* genome at the *rdxA* locus. (B) PCR of erythromycin resistant *H. pylori* isolates using

589 primers that flank the *rdxA* locus. The nomenclature above each band indicates the amplified product. (-

590); PCR no template control. *kan-sacB*; kanamycin resistance and sucrose sensitivity selection marker

591 present in the *H. pylori* transformation background and serves as a negative control. *tlpD*, ΔN4, ΔN5,

592 ΔC3, ΔC4 are the versions of *tlpD* on the cassette that were PCR amplified.

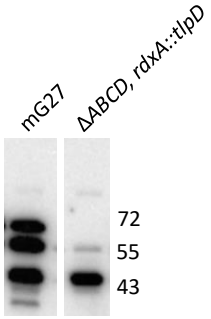

593

594 **Figure S4. TlpD is produced when complemented into *H. pylori* that lacks all chemoreceptors.** Western
595 blot of *H. pylori* mG27 *Δabcd* expressing complemented WT *tlpD* was analyzed from whole-cell lysates
596 with an anti-TlpA22 antibody which recognizes the MA domain. The strains analyzed are indicated at the
597 top. Marker sizes are given in kilodaltons on the right. The expected size of TlpD is 48 kDa. Western blot
598 is representative of 2 biological replicates.

Table S1. Primers used in this study.

Primer	Oligonucleotide sequence
rdxA Fwd	cgccattcttgcaagatgtttg
rdxA Rev	ctcgcttctgccaccctctt
tlpD pUT18 Fwd	agatCTGCAGatgtttgggaataagcagttac[a]
tlpD pUT18 Rev	ggagGGTACCttcgccttttttgaatttttttcaatg[a]
ΔC4 pUT18 Fwd	aattCTGCAGatgtttgggaataagcagttacagc[a]
ΔC4 pUT18 Rev	gagaGGTACCggtaatgtggtcttcttgaacg[a]

599 [a]Restriction sites are capitalized.

600 **File S1. TlpD secondary structure bioinformatic analysis.**
601 **File S2. *tlpD* plasmid sequences.**